Available online at www.sciencedirect.com
SCIENCE DIRECT®
C. R. Physique 6 (2005) 945–955
COMPTES RENDUS PHYSIQUE
http://france.elsevier.com/direct/COMREN/

Spintronics/Spintronique

# Spin dependent transport: GMR & TMR

Alain Schuhl *, Daniel Lacour

*LPM-UMR7556, faculté des sciences, université Henri-Poincaré Nancy-I, 54506 Vandœuvre les Nancy, France*

Available online 6 December 2005

**Abstract**

The discovery of giant magnetoresistance in 1988 opened the large research field of 'spintronics'. Twenty years later, a large number of devices makes use of the electron's spin, in addition to its charge, to control electronic transport properties. The physical origin of spintronic phenomena is the different conduction properties of the majority and minority spin electrons in a ferromagnetic metal. At an interface involving a ferromagnetic conductor, this leads to spin dependent conduction or tunneling properties. Here we present an overview of magnetotransport phenomena in structures involving metallic layers. ***To cite this article: A. Schuhl, D. Lacour, C. R. Physique 6 (2005).***


**Résumé**

**Transport dépendant du spin : la GMR et la TMR.** La découverte de la magnétorésistance géante dans les multicouches magnétiques a ouvert un nouveau champ de recherche : l'électronique de spin. Prés de 20 ans plus tard, les phénomènes de transport dépendant du spin sont utilisés dans de nombreux composants. La possibilité de contrôler le transport électronique non seulement par la charge mais aussi par le spin de l'électron introduit de nouveaux degrés de liberté. L'électronique de spin, exploite la sensibilité à la direction du spin électronique des propriétés de transport dans un métal ferromagnétique. Cela se traduit par une influence très importante de la direction du spin des électrons de conduction sur la résistance électrique à l'interface avec un autre matériau. Dans cet article nous décrivons les principaux phénomènes de transport dépendant du spin au travers de couches fines de matériaux ferromagnétiques dans les multicouches métalliques et dans les structures à barrière tunnel. ***Pour citer cet article : A. Schuhl, D. Lacour, C. R. Physique 6 (2005).***


*Keywords:* Magnetoresistance; Spin dependent transport; GMR; TMR

*Mots-clés :* Magnétorésistance ; Transport dépendant du spin ; GMR ; TMR

## 1. Introduction

The discovery of the giant magnetoresistance (GMR) of the magnetic multilayers in 1988 [1,2] opened the large research field of 'spintronics'. Then, during the two following decades, it has led to many solid state applications of spin dependent transport. The introduction of different conduction behavior for the majority and minority spin electrons in a ferromagnetic metal was first suggested fifty years before by Mott [3]. He pointed out that in ferromagnetic material, at sufficiently low temperatures, when the mean free path is long enough, electrons with magnetic moment parallel and antiparallel to the bulk magnetization do

* Corresponding author.
*E-mail address:* Schuhl@lpm.u-nancy.fr (A. Schuhl).

1631-0705/$ – see front matter 
doi:10.1016/j.crhy.2005.10.010

not mix in the scattering processes. The two spin channels contribute in parallel to conduction, and the conductivity is then the sum of two independent contributions. Known as the two-current model, this approach has been extended later in 1968 by Fert and Campbell [4]. The discovery of GMR triggered an extensive research effort on spin transport in magnetic nanostructures and other interesting effects rapidly appeared. One of the most important is the tunneling magnetoresistance (TMR) of magnetic tunnel junctions (MTJ). The first TMR experiment (at low temperature) actually dates back to 1975 [5] but it is only in 1995 [6] that the observation of large and reproducible effects kicked off the research effort on MTJ. A magnetic tunnel junction is composed of two ferromagnetic conducting layers separated by an ultrathin insulating layer. As in GMR, the resistance of the junction is linked to the relative orientation of electrodes' magnetization.

## 2. Giant Magnetoresistance

The Giant Magnetoresistance (GMR) was discovered by Baibich et al. [1] and simultaneously by Binash et al. [2] in 1988. In both cases, Fe/Cr (001) multilayers, either Fe/Cr (001) superlattices for the Orsay team or Fe/Cr/Fe(001) trilayers for the Jülich group, were grown by molecular beam epitaxy (MBE). In these structures, when the configuration of the magnetizations in the neighboring Fe layers goes from antiparallel to parallel alignment, a large resistance drop is observed. The variation of the resistance as a function of the magnetic field observed by Baibich et al. for Fe/Cr superlattices at 4.2 K is shown on Fig. 1. When the magnetic field is increased, the resistance drops as the configuration of the magnetizations in neighboring Fe layers goes from antiparallel to parallel. Since the reduction of the resistivity is significant, this effect has been called Giant Magnetoresistance or GMR.

The saturation field *Hs*, is the field required to overcome the antiferromagnetic interlayer coupling between the Fe layers and align the magnetizations of consecutive layers. In the first observations, in Fe/Cr multilayers, the value of *Hs* was very large, in the order of 1 Tesla. This was a strong handicap for the applications of this effect. However, as we will discuss below, rapidly after the discovery of GMR, new structures with low saturation field were achieved. The magnetoresistance ratio, defined as the ratio of the resistivity change to the resistivity in the parallel configuration:

$$MR = \frac{\rho_{AP} - \rho_P}{\rho_P}$$

reaches 80% at 4.2 K, for the sample with 9 Å thick Cr layers shown in Fig. 2 (and still 20% at room temperature). A record *MR* ratio of 220% has been obtained in 1994 again on Fe/Cr multilayers [7], which means that the conductivity is three time larger in parallel than in antiparallel configuration.

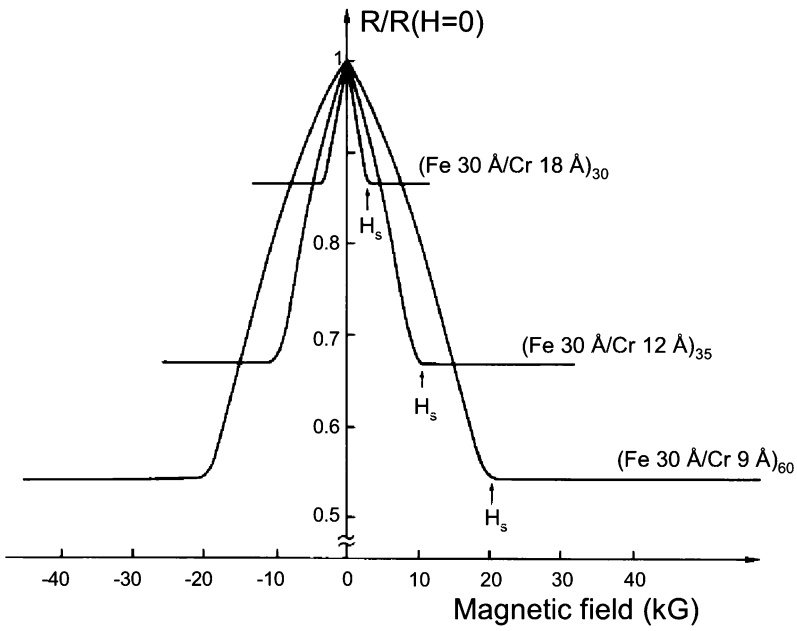


Fig. 1. Magnetoresistance curves at $T = 4.2$ K for Fe(001)/Cr(001) superlattices, from [1].

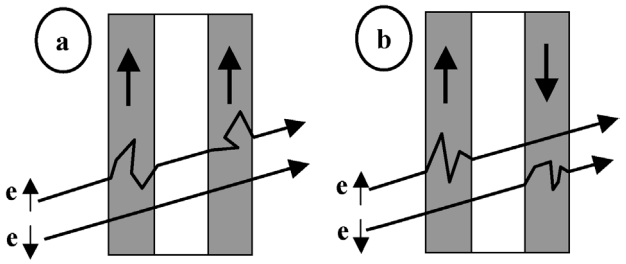


Fig. 2. Simplistic picture of spin dependent scattering for the explanation of the GMR effect. Only minority electrons are scattered. Unscattered majority electrons cause a short circuit effect, which appears for parallel alignment of the magnetizations (a) but not for antiparallel alignment (b).

### *2.1. Two current model*

The physical origin of GMR is the influence of the electron spin on the electronic transport in ferromagnetic conductors. As has been first proposed by Mott [3], the spin splitting of the energy bands in the ferromagnetic state leads to specific transport behavior. Then, the Fert and Campbell team in Orsay has demonstrated experimentally the spin dependence of the conduction in ferromagnetic metals and alloys by using a series of iron-based and nickel-based alloys [4,8]. These experimental results could be accounted for by the 'two current model' of conduction in ferromagnetic metals [4,8,9]. In the low temperature limit, when the spin flip scattering of the conduction electrons by magnons is frozen out, the spin mixing rate is much smaller than the momentum relaxation rate. Then there are two independent parallel channels for the electrical current: spin↑ (majority) and spin↓ (minority) electrons. The conductivity of the ferromagnet is then the sum of two independent contributions, and the resistivity can be expressed as:

$$\rho = \frac{\rho_\uparrow \rho_\downarrow}{\rho_\uparrow + \rho_\downarrow}$$

where $\rho_\uparrow$ ($\rho_\downarrow$) are the resistivities of the spin↑ (↓) channels, respectively.

There are several contributions to the difference between $\rho\uparrow$ and $\rho\downarrow$, either intrinsical related to the spin dependence of the electrical conductivity parameters $\sigma_\nu = n_\nu e^2 \tau_\nu / m_\nu$, where $\nu = \uparrow$ or $\downarrow$, where $\tau_\nu$ is the spin relaxation time, $m_\nu$ the effective mass, and $n(E_F)$ the density of states at the Fermi level $n_\nu(E_\mathrm{F})$, or extrinsical related to the spin dependence of the impurity or defect potential $V_\nu$ . The latter case has been experimentally pointed out by Fert and Campbell [4]. They have shown that the asymmetry ratio $\alpha$ of spin↑ and spin↓ resistivities, defined by

$$\alpha = \frac{\rho_\downarrow}{\rho_\uparrow}$$

can be as large as 20 for example, when 1% of Co or Fe impurities are introduced in a Ni sample. In the other hand, values of $\alpha$ smaller than 1 were obtained for Cr (or also V). This difference can be explained by the electronic structure of Cr impurities in Ni metallic lattice. The d-spin↑ energy levels of Cr are located above the d-spin↑ band of Ni. This prevents the hybridization of the d↑ states of Cr with the d↑ band of Ni. It is replaced by a hybridization with the s↑ band of Ni to form a virtual bound state at an energy close to the Fermi level. This leads to a strong scattering in the spin↑ channel and explains the higher mobility in the spin↓ channel for nickel with chromium impurities. In multilayers, important conductivity asymmetry can then be induced by the spin dependent scattering at the interfaces between, for example, Fe and Cr layers.

### *2.2. Giant magnetoresistance mechanism*

The main features of the GMR can be pointed out in the framework of the free electron model by using spin dependent scattering by the defects and impurities of the magnetic layers and by the roughness of their interfaces. In each magnetic layer the scattering probability is thus different for the majority and minority spin electrons. We consider here a thin nonmagnetic spacer in between two magnetic layers (Fig. 2), and we assume that the electron mean free path, for both spin directions, is much larger than the individual layer thickness, so that the scattering must be averaged over the entire structure. The conductance of the trilayer is then the sum of two independent contributions: the spin+ and the spin− channels.

In the parallel (P) configuration, the electrons of the spin+ channel are majority electrons in both magnetic layers, and indeed spin− are minority electrons in both magnetic layers. This gives different resistances $r_{\uparrow\uparrow}$ and $r_{\downarrow\downarrow}$ for the two channels and the resistance is then:

$$r_\mathrm{P} = \frac{r_{\uparrow\uparrow} \cdot r_{\downarrow\downarrow}}{r_{\uparrow\uparrow} + r_{\downarrow\downarrow}}$$

In the antiparallel (AP) configuration, electrons of both channels are alternatively majority and minority spin electrons and the shorting by one of the channels disappears. The resistance is then the same for both channels, $r_{\uparrow\downarrow} = r_{\downarrow\uparrow} = (r_{\uparrow\uparrow} + r_{\downarrow\downarrow})/2$, and the resistance is:

$$r_{\mathrm{AP}} = \frac{r_{\uparrow\uparrow} + r_{\downarrow\downarrow}}{4}$$

We thus obtain the following GMR ratio:

$$MR = \frac{r_{\mathrm{AP}} - r_{\mathrm{P}}}{r_{\mathrm{P}}} = \frac{(r_{\uparrow\uparrow} - r_{\downarrow\downarrow})^2}{4 r_{\uparrow\uparrow} r_{\downarrow\downarrow}}$$

If the spin diffusion is highly asymmetric (for example $r_{\uparrow\uparrow} < r_{\downarrow\downarrow}$), in the parallel configuration the current is shorted by the undiffused spin channel and the resistance is low ($r_{\mathrm{P}} \approx r_{\uparrow\uparrow}$), whereas in the antiparallel configuration both currents are limited by the diffusion in one of the layers and the resistance ($r_{\mathrm{AP}} \approx r_{\downarrow\downarrow}/4$) is much higher than in parallel configuration.

Camley and Barnas [10,11] have developed the first semi-classical model of GMR. It was based on the picture of free electrons scattered by a distribution of spin dependent centers that are affected by the magnetic configuration of the multilayer. Specular reflections by the interfaces have also been taken into account. This approach has been further developed in a large number of papers, and extensively applied to the interpretation of experimental data [12]. Analytical expressions of the GMR were derived by Barthélémy and Fert [13] in the simple case where the GMR comes only from interface scattering. It was found that, in the limit of thick nonmagnetic layers, the GMR ratio vanishes asymptotically as $\exp(-t_{\mathrm{nm}}/\lambda_{\mathrm{nm}})$, where $\lambda_{\mathrm{nm}}$ and $t_{\mathrm{nm}}$ are respectively the mean free path (MFP) and the thickness of the nonmagnetic spacer. Moreover, the GMR ratio is then expected to decrease more slowly with the thickness of ferromagnetic layer, since it varies as $\lambda_{\mathrm{F}}/t_{\mathrm{F}}$ when the thickness of the magnetic layers, $t_{\mathrm{F}}$, becomes much larger than $\lambda_{\mathrm{F}}$, the MFP in the magnetic layers. This is due to the fact that the conduction in a magnetic layer is affected by the orientation of the neighboring magnetic layers only within the depth $\lambda_{\mathrm{nm}}$ in which the electron retains the knowledge of its linear momentum. Phenomenologically simple expressions have also been derived by Dieny et al. [14]. Using the quantum-mechanical equation of motion of the density matrix, Levy et al. [15] developed a quantum model within the framework of the Kubo formalism. Apart from the quantum-size effects, the predictions of the quantum free electron models for the variations of the GMR versus layers thickness are in good agreement with the semiclassical results. Moreover, both fit reasonably well the experimental data. However, quantitative predictions of the amplitude of the GMR are difficult because the parameters controlling this amplitude are poorly known. For a realistic comparison with experimental results and quantitative predictions, it is necessary to introduce an accurate description of the spin-polarized band structure.

### *2.3. Antiferromagnetic alignment*

Although the first observation of GMR effect by Baibich et al. [1] and Binash et al. [2] were obtained on epitaxial samples, similar effects have been rapidly obtained on polycrystalline multilayers deposited by sputtering. In 1990, Parkin et al. [16] explored very broad thickness ranges for Fe/Cr, Co/Ru and Co/Cr multilayers. They have observed an oscillatory dependence of the magnetoresistance as the thickness of the nonmagnetic layer increases. This is a consequence of the oscillating behavior of the interlayer exchange coupling. Indeed, the GMR effect can be observed only when an antiparallel alignment of magnetic

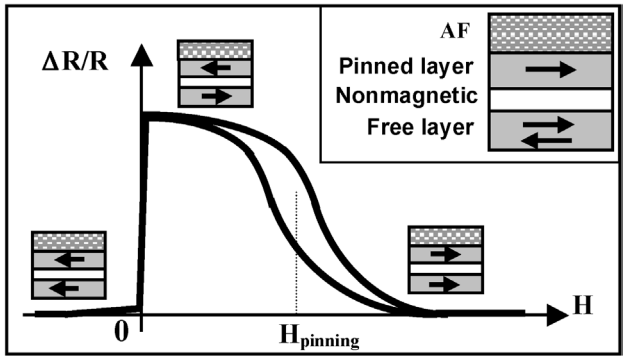


Fig. 3. Schematic picture of a spin valve structure and corresponding magnetoresistance loop at room temperature. Magnetic configuration of pinned and free layers are also indicated above the curve at three important stages of the loop: for $H < 0$ corresponding to a parallel alignment, for $0 < H < H_{\mathrm{pinning}}$ where the antiparallel magnetization configuration is achieved, and finally for $H > H_{\mathrm{pinning}}$ again corresponding to a parallel alignment.

layer can be achieved. So, GMR effects are observed in the thickness ranges where the coupling is antiferromagnetic (AF) and vanishes when the coupling is ferromagnetic (F). In 1991 is has been shown that Co/Cu multilayers also show oscillations of the exchange coupling [17,18]. With a very high GMR ratio, above 200%, this system rapidly became a multilayer model for GMR. The variation of the *MR* ratio as a function of the Cu thickness exhibits three well defined maxima associated with three ranges of antiferromagnetic coupling. As expected, the height of the maxima decreases exponentially with the thickness of the nonmagnetic spacer. Moreover, the GMR vanishes when the Cu thickness becomes larger than the electron mean free path in Cu.

Although it leads to a high magnetoresistance ratio, the use of AF interlayer exchange coupling in real devices is limited by the height of the magnetic field required to change the magnetic configuration. The antiparallel configuration and consequently GMR effects have also been obtained with multilayers combining two different magnetic materials [19]. The switching of the magnetizations of magnetic layers occurs at different fields: at low field for soft layers and at high field for hard layers. In the intermediate field range, where only one type of layer has been switched, an antiparallel alignment is achieved and the resistance is higher. For applications, it is important to achieve a large contrast in the field for the switching of magnetization of soft and hard layers, and simultaneously a very low switching field of the soft layer.

In Fig. 3 we show a simple picture of the 'spin-valve' structure first introduced in 1991 [20,21] and now used in most of applications, for example, in read head of hard disks. Its consist of a magnetically soft layer, separated by a nonmagnetic layer from a second magnetic layer, which has its magnetization pinned by an exchange biasing interaction with an antiferromagnetic (FeMn and now IrMn) or ferrimagnetic layer. When the magnetic field increases from negative to positive values, the magnetization of the unpinned or free layer reverses in a small field range close to $H = 0$, whereas the magnetization of the pinned layer remains fixed in the negative direction. Then, the resistance increases steeply in this small field range and consequently, the sensitivity of the device measured in %/Oe increases strongly [22]. However, the AF pinning 'spin-valve' is restricted to trilayer devices; it cannot be extended to multilayers, which show the highest GMR ratio. Nevertheless, it has been shown that by improving the electron specular reflectivity at the outer surfaces, a trilayer becomes equivalent to a multilayer [23]. The oxidation of a rough transition metal surface preferentially removes bumps and spikes, which are converted into an insulating oxide. Hence, the surface of the conducting layer becomes smoother. A spectacular increase of the GMR ratio due to this effect was recently obtained by Veloso et al. [24].

### *2.4. Spin accumulation and CPP GMR*

First observations of GMR were performed in the Current In Plane or CIP geometry, i.e. with the electrical current parallel to the plane of the layers. However, because of the symmetry of the current transport, it has been rapidly proposed to measure the spin dependent current with the Current Perpendicular to the Plane, that is called the CPP geometry. The first measurements in the CPP geometry have been performed at Michigan State University (MSU) [25] by sandwiching multilayers between two superconducting strips of Nb to produce uniform current density between the strips through the multilayer and measuring the voltage between the Nb strips. The detection of the very small resistive signal was detected by using a SQUID. A review of this

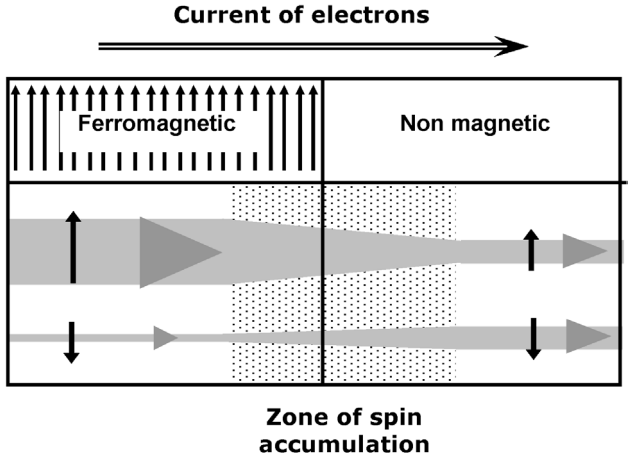


Fig. 4. At the interface between ferromagnetic and nonferromagnetic materials, the contribution of each spin channel changes. Consequently, some of the majority spins have to flip in order to insure current conservation. At this spin-flip time, we can associate a spin diffusion length. Due to the incoming and outgoing currents, in both sides of the interface, the density of spin↑ and spin↓ electrons is out of equilibrium; this effect is then called 'spin accumulation'.

type of measurement can be found in [26]. As expected, the magnetetoresistive signal is definitely larger in the CPP than in the CIP geometry.

Magnetoresistance in CIP and CPP measurement configurations involves significantly different physics. In CPP, the contribution of the specular reflections to resistivity leads to a spin dependent interface resistance [27] which introduces a spin dependent voltage drop between the two sides of an interface. Indeed, this effect does not appear when the current is parallel to the layers. However, the most important difference between the CIP and CPP is induced by the spin transport perpendicularly to an interface, which induces a spin accumulation effect. This effect is due to the fact that in a ferromagnetic material the difference between the conductivity of the two spin channels can be quite important. Suppose, as shown in Fig. 4, that an electrical current is crossing the interface between a nonmagnetic and a ferromagnetic layer. It corresponds to a flux of electrons going from the ferromagnetic to a nonmagnetic material. If, for example, the conductivity in the ferromagnetic material is larger for the majority spin electrons, the incoming electron flux is carried, in larger part, by the spin+ channel, while in the nonmagnetic layer both spin channels have an equivalent contribution to the current.

Let us consider now two ferromagnetic layers and in between a thin nonmagnetic spacer. We consider first the antiparallel configuration. When a current of electrons is going from layer with positive magnetization to the layer with negative magnetization, there is, in the central region, an accumulation of spin+ electrons and depletion of spin− electrons. Because of this out-of-equilibrium electron distribution, the number of spin flips increases and the system reach a steady state, which corresponds to a splitting of the chemical potentials of both spin directions. Since spin accumulation diffuses on distance of the order of the spin diffusion length (SDL) of the corresponding material, this effect spreads far away from the central region. According to the Valet and Fert model [28], the gradient of the spin dependent chemical potentials gives rise to spin dependent pseudo-electric fields that slow down the faster electrons, accelerate the slower ones and, on the whole, increase the effective resistivity in the spin accumulation zone. In parallel configuration, the spin accumulation is much smaller, because the same spin channel is dominant for electrical conductivity in both ferromagnetic films. The increase of resistivity is then smaller than in the antiparallel configuration, which corresponds to a significant GMR. Moreover, since the spin accumulation propagates over distances of the order of the SDL, which is much larger than the mean free path, the GMR subsists with very thick layers.

Experimentally, sizable CPP-GMR effects have observed for individual layer thicknesses in the micron range, first by the MSU group, and then by using multilayered nanowires electrodeposited into the pores of nuclear track-etched polycarbonate membranes [29]. The very high aspect ratio, with a length of 20–40 mm for a diameter in the range 30–100 nm, guarantees that the current is perpendicular to the layers.

## 3. Spin dependent tunneling

The spin asymmetry of density of state (DOS) in a ferromagnetic conductor leads not only to a spin dependent conduction but also to a spin dependent tunneling probability through a potential barrier. The tunneling magnetoresistance originates from this last property. The first observation and interpretation of spin dependent tunneling between two ferromagnetic electrodes was reported by Jullière in 1975 [5]. He was studying the magneto-transport properties of a magnetic tunnel junction composed of an oxidized Ge semiconductor layer separating Co and Fe ferromagnetic electrodes. Twenty years later, in 1995, a large effect at room temperature was observed [6]. This observation kicked off the tremendous research effort in this field. As in GMR, the resistance of the junction is linked to the relative orientation of the ferromagnetic electrodes magnetizations.

### *3.1. Jullière model*

The first TMR measurement in a Co/ oxidized Ge/ Fe MTJ was reported by Julière in 1975. At low temperature (4.2 K) and zero bias voltage, the conductance exhibits a variation of 14% between the antiparallel and the parallel alignment of the electrodes magnetization. The measured TMR was found to decrease and even vanish at increasing bias voltage (Fig. 5). In his article, Jullière proposed an interpretation taking into account the spin polarized tunneling effect. Assuming the tunneling process conserves the spin, the tunneling conductance can be considered as the sum of two independent conduction channels: one channel for each spin direction (Fig. 6). The relative variation of conductance and the DOS of each spin channel are then linked as follows in the Jullière formula:

$$TMR = \frac{2P_1P_2}{1 - P_1P_2}, \quad \text{where } P_i = \frac{D_{i\uparrow} - D_{i\downarrow}}{D_{i\uparrow} + D_{i\downarrow}}$$

and $D_1\uparrow(\downarrow)$ and $D_2\uparrow(\downarrow)$ are the DOS of the two ferromagnetic electrodes at the Fermi level for the two spin directions.

In 1995, the observation by two independent laboratories of high and reproducible TMR effects on MTJs at room temperature started the great research effort on MTJ. Moodera et al. at MIT and Miyazaki et al. in Sendai worked respectively on $CoFe/Al_2O_3/Co$ and $Fe/Al_2O_3/Fe$ MTJs, where the alumina barriers were amorphous [6]. One of the key parameters in these experiments was the growth of ultra thin tunneling barriers without any pinholes (metallic short circuits). Since then, an intense

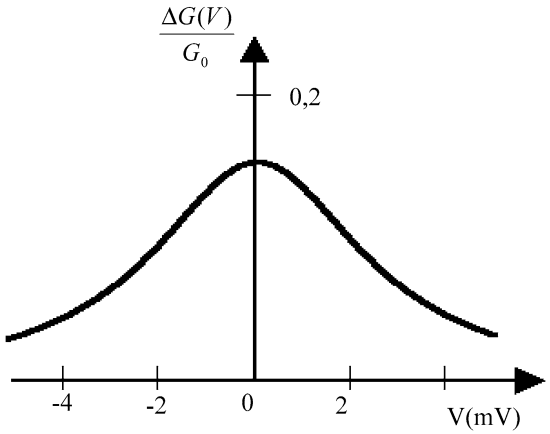


Fig. 5. First tunnel magnetoresistance observed at 4.2 K by Jullière in FeGeCo, from [5].

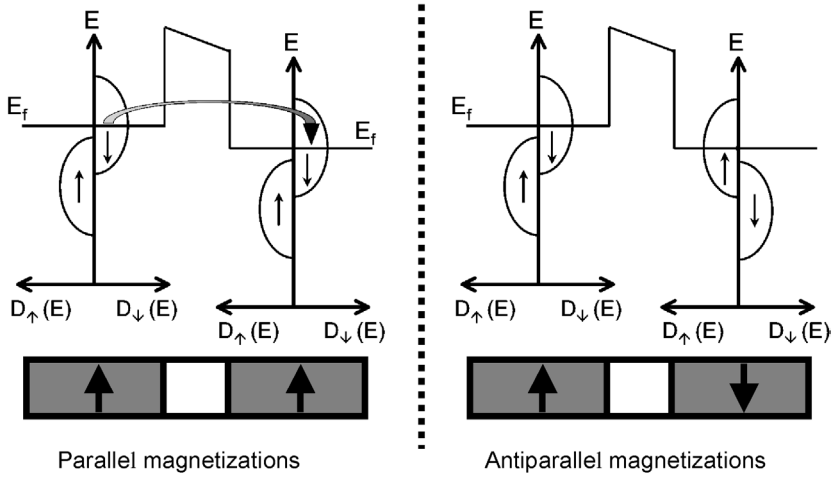


Fig. 6. Schematic density of states for both magnetic electrodes in the parallel (right) and antiparallel (left) configurations of magnetizations. In the Jullière model, the conductivity of each spin channel is proportional to both the spin DOS in the emitter and in the collector electrode. Consequently, the conductivity of the barrier, which is the sum of the two channel's conductivities is strongly dependent on the magnetization configuration.

research effort has been devoted to the increase of the TMR ratio. Various MTJs combining an amorphous barrier of alumina and Ni, Co, Fe and alloys of these metals have been tested. Sousa et al. have shown that an annealing of the multilayers under certain conditions almost doubles the TMR [30]. This effect has been attributed to a quality improvement of the amorphous barrier: a more homogeneous oxygen distribution within the barrier and sharper interfaces. The TMR ratio has been also enhanced by the use of polycrystalline CoFe [31] and amorphous CoFeB [32] electrodes leading respectively to a TMR of 50% and 70%. The magneto-transport properties of MTJs make them very attractive for at least two types of applications: the magnetic random access memories (MRAM) and the field sensors for read heads. These two applications require not only a high TMR but also submicrometer lateral sizes and a relatively low Resistance-Area product (RA): about 100 $\Omega\,\mu m^2$ for the first MRAM generation and less than 10 $\Omega\,\mu m^2$ for read heads sensors. Nanometer sized MTJ with various aspect ratios have been fabricated by electron beam lithography and intensively studied. To reach the low RA product required by the applications, important efforts have also been devoted to the tunneling barrier study. Various oxidation techniques have been developed and alumina barriers as thin as 0.7 nm have been obtained by in situ natural oxidation. The TMR ratio of these MTJs was equal to 20% while the RA product has been reduce down to 10 $\Omega\,\mu m^2$ [33]. An important effort has been also devoted to the research of an alternative insulating material. The main motivation was the reduction of the resistance of the tunnel junction and then the use of insulators with barrier heights lower than alumina. High TMR ratio have been obtained with many different barriers like $AlO_xN_y$ [34,35] $Ga_2O_3$ [36], $TaO_x$ [37], $ZrO_2$ [38] and $ZrAlO_x$ [39]. Beside the first motivation for increasing the performance of MTJ for applications, the achievement of good MTJ with different junction parameters is very important for building a spin transistor or spin diode using two or even more tunnel junctions [40].

### 3.2. Improvement of the TMR effect

Following the Jullière model, a simple way to increase the TMR is to use electrodes with higher spin polarization at the Fermi level. A fully polarized spin current is then expected as one electrode of the junction has a half-metallic behavior. Many candidates have been considered and studied, for example $CrO_2$, $Fe_3O_4$, $La_{0.7}Sr_{0.3}MnO_3$, $La_{0.7}Ca_{0.3}MnO_3$, $Sr_2FeMoO_6$ type, and Heusler alloys like NiMnSb or $Co_2MnSi$. Large TMR ratios have been obtained at low temperature for a few of these materials. However, this TMR vanishes below room temperature (RT). Bowen et al. [41] have observed very large TMR up to 1800% at low temperature. The TMR decreases to 30% at 250 K and vanishes at the effective Curie temperature about 300 K.

Up to now, most of the work on MTJ has been performed with an amorphous alumina barrier and recently monocrystalline MgO barrier. Since the tunnel current reveals the spin density of states of the electrodes, important information on the tunnel process has been obtained with some of the experiments made on MTJ with alternative barriers. De Teresa et al. [42] have pointed out the role of the barrier material on the spin dependent transport. They have shown that even the sign of the spin polarization of the tunneling electrons can change by modifying the barrier material. They studied $SrTiO_3$, $Ce_{0.85}La_{0.15}O_3$ and $Al_2O_3$ insulating layers or $SrTiO_3/Al_2O_3$ double barrier as insulating material (I), in $La_{0.7}Sr_{0.3}MnO_3$/I/Co multilayers. The half-metallic, $La_{0.7}Sr_{0.3}MnO_3$ manganite collects only electrons with their spin polarization parallel to its majority spin direction. In parallel magnetic configuration, it corresponds to majority spins of the cobalt, and to minority spins in antiparallel configuration. With an $Al_2O_3$ barrier the TMR found is normal, the resistance of the junction is higher in AP than in P configuration. These results are in agreement with a positive spin polarization for cobalt, as is commonly observed with an alumina barrier. On the other hand, the inverse TMR effect is observed when $SrTiO_3$ is used for the barrier. So, the electronic structure of the electrode/barrier interfaces plays an important role on the spin dependent tunnel conductivity. In recent experiments, negative spin polarization has also been found for Co with a $TiO_2$ barrier and for Ni with $SrTiO_3$ [43]. Sun et al. [44] have shown that chemical instabilities can change the sign of the spin polarization of Fe and Co with a $SrTiO_3$ barrier.

### 3.3. Free electron models

In 1989, Slonczewski extended the previously described model to the free electron framework [45]. He considered a rectangular potential barrier of height $V_B$ sandwiched between two similar and semi-infinite ferromagnetic electrodes. The ferromagnet properties of the electrodes were taken into account by the introduction of a molecular field. The spin polarization $P$ is then given by:

$$P = \frac{(k_\uparrow - k_\downarrow)}{(k_\uparrow + k_\downarrow)} \frac{(\kappa^2 - k_\uparrow k_\downarrow)}{(\kappa^2 + k_\uparrow k_\downarrow)}$$

where k↑(↓) represents the majority and minority Fermi momentum for the two ferromagnetic electrodes and $\kappa = \sqrt{(2m/\hbar^2)(V_B - E_F)}$ is the decay constant of the wave function in the barrier region for $k_\parallel = 0$. Note that the Slonczewski expression of the spin polarization is equivalent to the Jullière one in the limit of an infinite barrier height. In 1999, Zhang and Levy indicated the close link between the potential profile and the TMR effect [46]. Two years later, Montaigne et al. have addressed the case of asymmetric tunnel barrier within the free electron model. They showed that asymmetries in the TMR(V) curves could be related to the shape of the barrier [47]. The developed model reproduces both the bias voltage dependence of the TMR and the oscillations of TMR at high voltage.

### 3.4. Symmetry effects and spin filtering

In highly textured materials, the different tunneling mechanisms and symmetry-related decay rates of the Bloch waves for the majority and the minority spin channels should lead to very high TMR ratios. The first experimental results were obtained in a pioneering work by Bowen et al. [48] on single-crystalline Fe/MgO/FeCo(001). Then, the filtering effect has been experimentally shown by Faure-Vincent et al. [49,50]. With the same Fe/MgO/F(001) multilayer, but deposited by MBE on single crystalline MgO substrate, they obtained a tunnel magnetoresistance up to 100% at room temperature. More recently, also by using MBE growth of single-crystal Fe/MgO/Fe(001) structure, Yuasa et al. [51] have measured a TMR up to 250% at low temperature and 180% at RT. Simultaneously, TMR of 300% at low temperature and 220% at RT have been achieved after thermal annealing, by Parkin et al. [52] for CoFe/MgO/CoFe polycrystalline MTJ, deposited by sputtering. Moreover, with CoFeB/MgO/CoFeB MTJ grown by sputtering in which the MgO barrier is (001) textured but CoFeB amorphous, Djayaprawira et al. [53] found a TMR of 300% at low temperature and 230% at RT.

The importance of the symmetry in the tunneling barrier has been clearly emphasized by Mavropoulos et al. [54]. Evanescent DOS is taken into account through Bloch waves with a complex wave vector $k = q + i\kappa$. Here, the imaginary part of $k$ describes the decay of the wave function in the tunnel barrier. Junctions with an MgO barrier have been intensively investigated from the

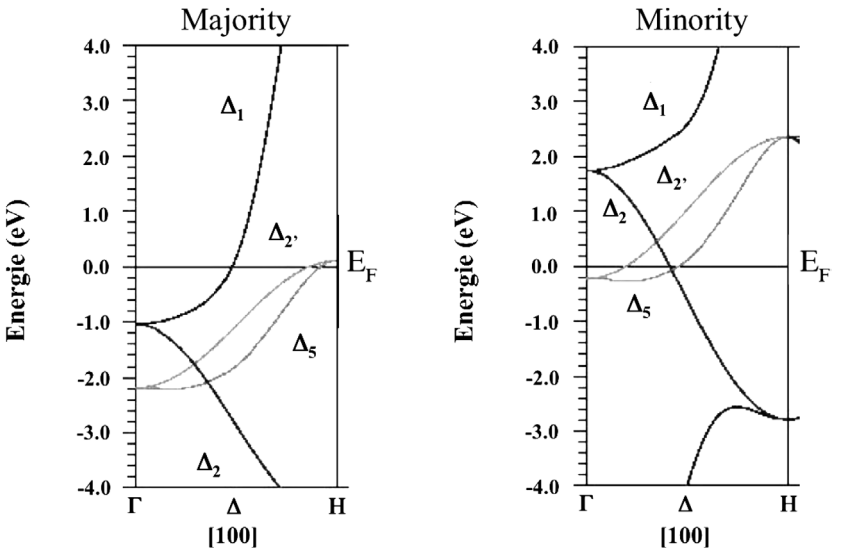


Fig. 7. Energy bands for the majority and minority spins in bcc Fe in the $\Delta = \Gamma - H$ direction. The band $\Delta_1$, $\Delta_5$ and $\Delta_{2'}$ have respectively 'spd', 'pd' and 'd' character state.

theoretical point of view, for example by Umerski and Mathon [55], and by Butler et al. [56,57]. In this system, because both materials (Fe and MgO) have roughly the same crystalline symmetry and the same parameters, the symmetry of the electronic bands are identical for all the structure: $\Delta_1$ with 'spd' character state, $\Delta_5$, with 'pd' character and a $\Delta_{2'}$ with 'd' character. The decay rate of the wave function in the barrier, measured by $\kappa$, is much stronger for $\Delta_5$ than the $\Delta_{2'}$ symmetry than for the $\Delta_1$ state.

The filtering effect can be easily understood if we suppose that the tunneling current is predominantly carried by electrons states which propagate along the (100), with their wave vector perpendicular to the interface direction, i.e. in the crystal $\Delta = \Gamma - \mathrm{H}$ direction. Fig. 7 presents the band structure of bulk-Fe in the 100 direction computed by Tiusan [58] using the Full Potential-Linear Augmented Plane Wave (FP-LAPW) Wien2k code [59]. It appears clearly that one of the spin directions is predominant at the Fermi level for the $\Delta_1$ symmetry. For large MgO thickness, in the parallel (P) configuration, the tunneling is found to be governed by the $\Delta_1$ state, because the other symmetries have a stronger attenuation rate. However, in the antiparallel configuration, a $\Delta_1$ state in the injection electrode cannot find an equivalent symmetry in the collector electrode, since its magnetization is reversed. The conduction is then driven predominantly by the $\Delta_5$ states propagation. The magnetoresistance is expected to be very high above 1000%. For low MgO thickness, the TMR ratio decreases because the contribution of $\Delta_5$ and $\Delta_{2'}$ bands becomes more and more significant.

### *3.5. Impurities, defects and surface states*

Even for the epitaxial tunnel junction, the transport phenomena can be strongly affected by the presence of several types of defects in the barrier or close to the barrier. On a first approach, the TMR ratio is expected to decrease, because the presence of defects like interface roughness, interdiffused interfaces, impurities or vacancies, or stacking faults, would provide additional conduction channels. This occurs not only with interfacial disorder but also with bulk defects. It has been shown that the introduction of some disorder within 10 ML of the electrode adjacent to the interface can reduce significantly the spin polarization of the tunneling [60]. The presence of localized defects and impurities inside the insulating barrier introduces a channel of impurity-assisted tunneling [61]. Beside the performance decrease of the spin dependent transport, the tunnel transmission is strongly affected by resonant effects at the interfaces. Each electron symmetry may then couple to one another, leading to a resonant tunneling mechanism [62]. Consequently a distribution of the impurity energy levels would lead to complex variations of the TMR with bias voltage and even inversions of the TMR. Improvement of the TMR ratio, for example at high voltages, has also been predicted. The role of the interface structure has been clearly shown in the experiments of LeClair et al. [63]. In tunnel junctions with amorphous barriers like alumina, the situation is even more complicated and is therefore hardly accessible to theory. This is due to multiple resonant scattering processes by several localized states and the resulting interferences. In this case Tsymbal and Pettifor [64] predicted a reduction of the TMR. In agreement with local measurements of the tunnel conductance by Da Costa et al. [65], the current as expected flows through a few regions corresponding to highly conducting channels induced by local disorder.

## 4. Perspectives

Ten years after the GMR discovery, all hard disk drives included GMR-based read heads. This has led to a significant improvement in the storage density and has demonstrated the potential of applications based on spintronics. Nonvolatile random access magnetic memories including MTJs as the storage element could be another great application of spintronics. Actually their low power consumption, their high scalability and their nonvolatility place them in a good position on the random access memory market with respect to semiconductor-based memories. Magnetic sensors, based on GMR and TMR detecting elements, have also been realized in the automotive industry for angle and position detection. High level of integration with the semiconductor industry will lead to low-cost fully integrated devices. Such magnetic sensors are also currently studied for Biochips applications. On the other hand, since reprogrammable logic devices using spin dependent transport are also in development, one could then imagine many low cost applications for complete devices, i.e. the sensor including its proximity logic, made by using only tunnel junction technology. Spin dependent transport in hybrid structures has not been discussed in this article. Nevertheless, similar spin dependent effect will lead to new devices. If a magnetic semiconductor could be used as a robust spin injector (spin aligner) into a nonmagnetic semiconductor, it would facilitate the integration of spintronics and semiconductor-based electronics. For example, Spin-LEDs allow modulating the light polarization by changing the magnetization direction of one active layer. Because the spin diffusion length is much larger in semiconductors than in conductors, the spin information could be propagated far away from the spin injector. Last, but not least, will be the use of the spin degree of freedom in molecular electronics. In the last years a number of recent advances have been made in this field: measurements performed on single molecules and demonstrations that molecules can exhibit diode and transistor behaviors. It has been recently shown [66] that low-energy electrons can traverse the molecular barrier while remaining spin polarized.

## References

[1] M.N. Baibich, J.M. Broto, A. Fert, F. Nguyen Van Dau, F. Petroff, P. Etienne, G. Creuzet, A. Friederich, J. Chazelas, Phys. Rev. Lett. 61 (1988) 2472.
[2] G. Binash, P. Grünberg, F. Saurenbach, W. Zinn, Phys. Rev. B 39 (1989) 4828.
[3] N.F. Mott, Proc. Roy. Soc.London Ser. A 153 (1936) 699.
[4] A. Fert, I.A. Campbell, Phys. Rev. Lett. 21 (1968) 1190;
A. Fert, I.A. Campbell, J. Physique 32 (C1) (1971) 46.
[5] M. Jullière, Phys. Lett. A 54 (1975) 225;
M. Jullière, Thesis of Rennes University, No. B368/217, Rennes, 1975.
[6] T. Miyazaki, N. Tezuka, J. Magn. Magn. Mater. 139 (1995) L231.
[7] R. Schad, C.D. Potter, P. Beliën, G. Verbanck, V.V. Moshchalkov, Y. Bruynseraede, Appl. Phys. Lett. 64 (1994) 3500.
[8] A. Fert, I.A. Campbell, J. Phys. F 6 (1976) 849.
[9] S. Maekawa, T. Shinjo (Eds.), Spin Dependent Transport in Magnetic Nanostructures, Taylor and Francis, 2002.
[10] R.E. Camley, J. Barnas, Phys. Rev. Lett. 63 (1989) 664.
[11] J. Barnas, A. Fuss, R.E. Camley, P. Grünberg, W. Zinn, Phys. Rev. B 42 (1990) 8110.
[12] B. Dieny, P. Humbert, V.S. Speriosu, S. Metin, B.A. Gurney, P. Baumgart, H. Lefakis, Phys. Rev. B 45 (1992) 806;
J. Barnas, A. Fuss, R.E. Camley, P. Grünberg, W. Zinn, Phys. Rev. B 42 (1990) 8110;
R.Q. Hood, L.M. Falicov, Phys. Rev. B 46 (1992) 8287;
V.V. Ustinov, E.A. Kravtsov, J. Magn. Magn. Mater. 148 (1995) 307;
L.G. Pereira, J.L. Duvail, D.K. Lottis, J. Appl. Phys. 88 (2000) 4772.
[13] A. Barthélémy, A. Fert, Phys. Rev. B 43 (1991) 13124.
[14] B. Dieny, P. Humbert, V.S. Speriosu, S. Metin, B.A. Gurney, P. Baumgart, H. Lefakis, Phys. Rev. B 45 (1992) 806.
[15] P.M. Levy, S. Zhang, A. Fert, Phys. Rev. Lett. 65 (1990) 1643.
[16] S.S.P. Parkin, N. More, K.P. Roche, Phys. Rev. Lett. 64 (1990) 2304.
[17] D.H. Mosca, F. Petroff, A. Fert, P.A. Schroeder, W.P. Pratt, R. Loloee, J. Magn. Magn. Mater. 94 (1991) L1.
[18] S.S.P. Parkin, R. Bhadra, K.P. Roche, Phys. Rev. Lett. 66 (1991) 2152.
[19] J. Barnas, A. Fuss, R.E. Camley, P. Grünberg, W. Zinn, Phys. Rev. B 42 (1990) 8110;
T. Shinjo, H. Yamamoto, J. Phys. Soc. Jpn. 59 (1990) 3061;
D.H. Mosca, F. Petroff, A. Fert, P.A. Schroeder, W.P. Pratt, R. Loloee, J. Magn. Magn. Mater. 94 (1991) L1;
S.S.P. Parkin, R. Bhadra, K.P. Roche, Phys. Rev. Lett. 66 (1991) 2152.
[20] B. Dieny, V.S. Speriosu, S.S.P. Parkin, B.A. Gurney, D.R. Wilhoit, D. Mauri, Phys. Rev. B 43 (1991) 1297.
[21] B. Dieny, V.S. Speriosu, J.P. Nozières, B.A. Gurney, A. Vedyayev, N. Ryzhanova, in: Proc. NATO ARW on Structure and Magnetism in Systems of Reduced Dimensions, in: NATO ASI Ser. B: Physics, vol. 309, Plenum Press, New York, 1993, p. 279.
[22] R. Coehoorn, in: K.H.J. Buschow (Ed.), in: Handbook of Magnetic Materials, vol. 5, Elsevier, 2003 (Chapter 1).
[23] W.F. Egheloff, et al., J. Appl. Phys. 79 (1996) 8603.
[24] A. Veloso, et al., Appl. Phys. Lett. 77 (2000) 1020.

[25] W.P. Pratt, S.F. Lee, J.M. Slaughter, R. Loloee, P.A. Schroeder, J. Bass, Phys. Rev. Lett. 66 (1991) 3060.
[26] J. Bass, W.P. Pratt Jr., J. Magn. Magn. Mater. 200 (1999) 274.
[27] J.J. Barnas, A. Fert, Phys. Rev. B 49 (1994) 12835;
B. Dieny, A. Granovsky, A. Vedyayev, N. Ryzhanova, C. Cowache, L.G. Pereira, J. Magn. Magn. Mat. 151 (1995) 378;
K.M. Schep, J.B.A.N. van Hoof, P.J. Kelly, G.E.W. Bauer, J.E. Inglesfield, Phys. Rev. B 57 (1998) 8907;
J. Chen, T.-S. Choy, J. Herschfield, J. Appl. Phys. 85 (1999) 4551;
M.D. Stiles, D.R. Penn, Phys. Rev. B 61 (2000) 3200;
J. Barnas, A. Fert, J. Magn. Magn. Mater. 136 (1994) 260;
S. Zhang, P.M. Levy, Phys. Rev. B 57 (1998) 5336;
K. Xia, P.J. Kelly, G.E.W. Bauer, I. Turek, J. Kudrnovsky, V. Drchal, Phys. Rev. B 63 (2001) 064407.
[28] T. Valet, A. Fert, Phys. Rev. B 48 (1993) 7099.
[29] L. Piraux, J.M. George, J.F. Despres, C. Leroy, E. Ferain, R. Legras, K. Ounadjela, A. Fert, Appl. Phys. Lett. 65 (1994) 2484;
A. Blondel, J.P. Meier, B. Doubin, J.Ph. Ansermet, Appl. Phys. Lett. 65 (1994) 3019.
[30] R.C. Sousa, J.J. Sun, V. Soares, P.P. Freitas, A. Kling, M.F. da Silva, J.C. Soares, Appl. Phys. Lett. 73 (1998) 3288.
[31] X.F. Han, M. Oogane, H. Kubota, Y. Ando, T. Miyazaki, Appl. Phys. Lett. 77 (2000) 283.
[32] D. Wang, C. Nordman, J.M. Daughton, Z. Qian, J. Fink, IEEE Trans. Magn. 40 (2004) 2269.
[33] Z.G. Zhang, P.P. Freitas, A.R. Ramos, N.P. Barradas, J.C. Soares, Appl. Phys. Lett. 79 (2001) 2219.
[34] M. Sharma, J.H. Nickel, T.C. Anthony, S.X. Wang, Appl. Phys. Lett. 77 (2000) 2219.
[35] J. Wang, P.P. Freitas, P. Wei, N.P. Barradas, J.C. Soares, J. Appl. Phys. 89 (2001) 6868.
[36] Z. Li, C. de Groot, J.S. Moodera, Appl. Phys. Lett. 77 (2000) 3630.
[37] P. Rottlander, M. Hehn, O. Lenoble, A. Schuhl, Appl. Phys. Lett. 78 (2001) 3274.
[38] J. Wang, P.P. Freitas, E. Snoeck, P. Wei, J.C. Soares, Appl. Phys. Lett. 79 (2001) 4387.
[39] J. Wang, P.P. Freitas, E. Snoeck, Appl. Phys. Lett. 79 (2001) 4553.
[40] M. Hehn, F. Montaigne, A. Schuhl, Phys. Rev. B 66 (2002) 144411.
[41] M. Bowen, M. Bibes, A. Barthélémy, J.-P. Contour, A. Anane, Y. Lemaitre, A. Fert, Appl. Phys. Lett. 82 (2003) 233.
[42] J.M. De Teresa, A. Barthélémy, A. Fert, J.P. Contour, F. Montaigne, A. Vaurès, Science 286 (1999) 507;
J.M. De Teresa, A. Barthélémy, A. Fert, J.P. Contour, R. Lyonnet, F. Montaigne, P. Seneor, A. Vaurès, Phys. Rev. Lett. 82 (1999) 4288.
[43] M. Bibes, M. Bowen, A. Barthélémy, A. Anane, K. Bouzehouane, C. Carrétéro, P. Contour, O. Durand, Appl. Phys. Lett. 82 (2003);
A. Fert, A. Barthélémy, J. Ben Youssef, J.P. Contour, V. Cros, J.M. de Teresa, A. Hamzic, J.M. George, G. Faini, J. Grollier, H. Jaffrès, H. Le Gall, F. Montaigne, F. Pailloux, F. Petroff, Mater. Sci. Eng. B 84 (2001) 1.
[44] J.Z. Sun, K.P. Roche, S.S.P. Parkin, Phys. Rev. B 61 (2000) 11244.
[45] J.C. Slonczewski, Phys. Rev. B 39 (1989) 6995.
[46] S. Zhang, P.M. Levy, Eur. Phys. J. B 10 (1999) 599.
[47] F. Montaigne, M. Hehn, A. Schuhl, Phys. Rev. B 64 (2001) 144402.
[48] M. Bowen, V. Cros, F. Petroff, A. Fert, C. Martínez Boubeta, J.L. Costa-Krämer, J.V. Anguita, A. Cebollada, F. Briones, J.M. de Teresa, L. Morellón, M.R. Ibarra, F. Güell, F. Peiró, A. Cornet, Appl. Phys. Lett. 79 (2001) 1655.
[49] J. Faure-Vincent, C. Tiusan, E. Jouguelet, F. Canet, M. Sajieddine, C. Bellouard, E. Popova, M. Hehn, F. Montaigne, A. Schuhl, Appl. Phys. Lett. 82 (2003) 4507.
[50] J. Faure-Vincent, Ph.D., Université Henri Poincarré, Nancy, 2004.
[51] S. Yuasa, T. Nagahama, A. Fukushima, Y. Suzuki, K. Ando, Nature Mater. 3 (2004) 868.
[52] S.S.P. Parkin, C. Kaiser, A. Panchula, P.M. Rice, B. Hughes, M. Samant, S.H. Yang, Nature Mater. 3 (2004) 862.
[53] D.D. Djayaprawira, K. Tsunekawa, M. Nagai, H. Maehara, S. Yamagata, N. Watanabe, S. Yuasa, Y. Suzuki, K. Ando, Appl. Phys. Lett. 86 (2005) 092502.
[54] Ph. Mavropoulos, N. Papanikolaou, P.H. Dederichs, Phys. Rev. Lett. 85 (2000) 1088.
[55] J. Mathon, A. Umerski, Phys. Rev. B 60 (1999) 1117.
[56] J.M. MacLaren, X.-G. Zhang, W.H. Butler, X. Wang, Phys. Rev. B 59 (1999) 5470.
[57] W.H. Butler, X.-G. Zhang, T.C. Schulthess, J.M. MacLaren, Phys. Rev. B 63 (2001) 054416.
[58] C. Tiusan, J. Phys.: Condens. Matter (2005), submitted for publication.
[59] P. Blaha, K. Schwarz, G.K.H. Madsen, D. Kvasnicka, J. Luitz, WIEN2k, An Augmented Plane Wave + Local Orbitals Program for Calculating Crystal Properties (K. Schwartz, Techn. Univ. Wien, Austria), 2001. ISBN 3-9501031-1-2.
[60] E.Y. Tsymbal, I.I. Oleinik, D.G. Pettifor, J. Appl. Phys. 87 (2000) 5230.
[61] E.Y. Tsymbal, A. Sokolov, I.F. Sabirianov, B. Doudin, Phys. Rev. Lett. 90 (2003) 186602.
[62] O. Wunnicke, N. Papanikolaou, R. Zeller, P.H. Dederichs, V. Drchal, J. Kudrnovsky, Phys. Rev. B 65 (2002) 064425.
[63] P. LeClair, H.J.M. Swagten, J.T. Kohlhepp, R.J.M. Van de Veerdonk, W.J.M. de Jonge, Phys. Rev. Lett. 84 (2000) 2933;
P. LeClair, J.T. Kohlhepp, H.J.M. Swagten, W.J.M. de Jonge, Phys. Rev. Lett. 86 (2001) 1066.
[64] V. Da Costa, C. Tiusan, T. Dimopoulos, K. Ounadjela, Phys. Rev. Lett. 85 (2000) 876.
[65] E.Y. Tsymbal, D.G. Pettifor, Phys. Rev. B 58 (1998) 432;
E.Y. Tsymbal, D.G. Pettifor, J. Magn. Magn. Mater. 199 (1999) 146;
E.Y. Tsymbal, D.G. Pettifor, J. Appl. Phys. 85 (1999) 5801.
[66] J.R. Petta, S.K. Slater, D.C. Ralph, Phys. Rev. Lett. 93 (2004) 136601.